Potential benefits of free-form optics in on-axis imaging applications with high aspect ratio

Fabian Duerr,* Youri Meuret, and Hugo Thienpont

Brussels Photonics Team, Vrije Universiteit Brussel, Pleinlaan 2, B-1050 Brussels, Belgium

*fduerr@b-phot.org

Abstract: Including free-form optical components in imaging systems provides numerous opportunities for enhanced performance and compact, lightweight packaging. This applies especially to the use of free-form optics in off-axis imaging applications. In case of on-axis imaging, rotationally symmetric lenses are typically used, as they greatly simplify the design and manufacturing process. However, for imaging applications with high aspect ratio, free-form optics can help to provide solutions with clearly better overall imaging performance. For such cases, the ray tracing simulations in this work demonstrate superior imaging performance of basic free-form lenses in comparison to conventional rotationally symmetric lenses, each consisting of two surfaces.

OCIS codes: (080.2720) Mathematical methods (general); (080.2740) Geometric optical design; (080.3620) Lens system design; (080.4225) Nonspherical lens design.

References and links

1. J. Rolland and K. Thompson, "Freeform optics: Evolution? no, revolution!" SPIE Newsroom (19 July 2012).
2. W. T. Plummer, "Unusual optics of the Polaroid SX-70 land camera," Appl. Opt. **21**, 196–208 (1982).
3. W. T. Plummer, J. G. Baker, and J. Van Tassell, "Photographic optical systems with nonrotational aspheric surfaces," Appl. Opt. **38**, 3572–3592 (1999).
4. O. Cakmakci and J. Rolland, "Design and fabrication of a dual-element off-axis near-eye optical magnifier," Opt. Lett. **32**, 1363–1365 (2007).
5. O. Cakmakci, B. Moore, H. Foroosh, and J. Rolland, "Optimal local shape description for rotationally nonsymmetric optical surface design and analysis," Opt. Express **16**, 1583–1589 (2008).
6. T. Nakano and Y. Tamagawa, "Configuration of an off-axis three-mirror system focused on compactness and brightness," Appl. Opt. **44**, 776–783 (2005).
7. J. M. Rodgers, "Catoptric optical system including concave and convex reflectors," (1994). US Patent 5,309,276.
8. K. Fuerschbach, J. Rolland, and K. Thompson, "A new family of optical systems employing φ-polynomial surfaces," Opt. Express **19**, 21919–21928 (2011).
9. R. Shack and K. Thompson, "Influence of alignment errors of a telescope system on its aberration field," Proc. SPIE **251**, 146–153 (1980).
10. K. Thompson, T. Schmid, O. Cakmakci, and J. Rolland, "Real-ray-based method for locating individual surface aberration field centers in imaging optical systems without rotational symmetry," JOSA A **26**, 1503–1517 (2009).
11. T. Schmid, J. P. Rolland, A. Rakich, and K. P. Thompson, "Separation of the effects of astigmatic figure error from misalignments using Nodal Aberration Theory (NAT)," Opt. Express **18**, 17433–17447 (2010).
12. P. Benítez and J. C. Miñano, "Ultrahigh-numerical-aperture imaging concentrator," J. Opt. Soc. Am. A **14**, 1988–1997 (1997).
13. J. C. Miñano, P. Benítez, W. Lin, J. M. Infante, F. Muñoz, and A. Santamaría, "An application of the SMS method for imaging designs," Opt. Express **17**, 24036–24044 (2009).
14. J. M. Infante Herrero, F. Muñoz, P. Benítez, J. C. Miñano, L. Wang, J. Vilaplana, G. Biot, and M. de La Fuente, "Novel fast catadioptric objective with wide field of view," Proc. SPIE **7787**, 778704 (2010).

#200472 - $15.00 USD Received 31 Oct 2013; revised 26 Nov 2013; accepted 26 Nov 2013; published 9 Dec 2013

15. W. Lin, P. Benítez, J. C. Miñano, J. M. Infante, and G. Biot, "Advances in the SMS design method for imaging optics," Proc. SPIE **8167**, 81670M (2011).
16. W. Lin, P. Benítez, J. C. Miñano, J. M. Infante, G. Biot, and M. de la Fuente, "SMS-based optimization strategy for ultra-compact SWIR telephoto lens design," Opt. Express **20**, 9726–9735 (2012).
17. F. Duerr, P. Benítez, J. C. Miñano, Y. Meuret, and H. Thienpont, "Analytic design method for optimal imaging: coupling three ray sets using two free-form lens profiles," Opt. Express **20**, 5576–5585 (2012).
18. F. Duerr, P. Benítez, J. C. Miñano, Y. Meuret, and H. Thienpont, "Analytic free-form lens design in 3D: coupling three ray sets using two lens surfaces," Opt. Express **20**, 10839–10846 (2012).
19. *CODE V Reference Manual* (Synopsis, 2011), chap. 18: Automatic Design in CODE V, pp. 18.1–18.50.
20. O. Cakmakci, J. Rolland, K. Thompson, and J. Rogers "Design efficiency of 3188 optical designs," Proc. SPIE **7060**, 70600S (2008).
21. J. Liu, J. C. Miñano, P. Benítez, and W. Lin, "Single optical surface imaging designs with unconstrained object to image mapping," Proc. SPIE **8550**, 855011 (2012).

1. Introduction

For decades, established manufacturing techniques for highly accurate lens surfaces in glass were restricted to rotationally symmetric spherical surfaces for accuracy and economic reasons. This restriction has largely been eliminated by the development of high precision single-point diamond turning and mass-replication technology, along with the increasing use of plastics for optical components. These recent advances in free-form tooling are rapidly changing the field of optics manufacturing which allow increasingly precise fabrication of surfaces with almost any shape. By removing restrictions on surface geometry, free-form optics help to develop increasingly compact yet better performing optical systems [1].

1.1. Benefits of free-form optics solutions in off-axis designs

Off-axis optical designs allow to make the optical systems smaller, thinner and lighter compared with conventional coaxial optics designs. The Polaroid SX-70 camera, introduced in 1972, was one of the first successful commercial products that used free-form surfaces to provide a well-corrected off-axis imaging system design, even though the term free-form was not yet established [2, 3]. Free-form optics can be also used to improve the state-of-the-art in catadioptric magnifiers with a dual-element off-axis magnifier [4]. The use of tilted mirror designs allow to dramatically increase the field of view and speed of an optical system [5]. Unobscured off-axis three- and four-mirror systems have been thoroughly studied in the past, e.g. by Nakano [6]. Figure 1 (left) shows an optical system designed and patented by Rodgers in 1994 [7]. At that time, it had the largest planar, circular input aperture in the smallest overall spherical volume. The design uses off-axis sections of rotationally symmetric conic mirrors.

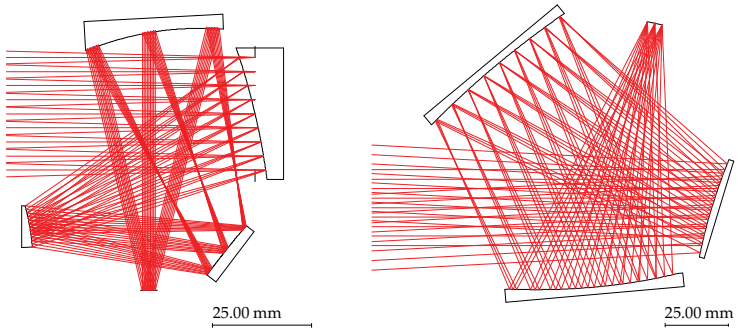

Fig. 1. (Left) Layout of U.S. Patent 5,309,276 consisting of three off-axis sections of rotationally symmetric mirrors and a fourth fold mirror [7]. (Right) A new free-form optical design based on tilted ϕ-polynomial surfaces (images source: Fuerschbach et al. [8]).

#200472 - $15.00 USD Received 31 Oct 2013; revised 26 Nov 2013; accepted 26 Nov 2013; published 9 Dec 2013

The system on the right shows a three-mirror system using tilted free-form optical surfaces designed by Fuerschbach et al. in 2011 [8]. The design of this free-form system is based on optimization strategies that make use of nodal aberration theory developed by Shack, Thompson and Schmid [9–11]. Their free-form optical system provides diffraction limited performance and extends the usable field by an order of magnitude in area [8], clearly emphasizing the benefits of free-form optics in off-axis designs.

1.2. A need for free-form optics in on-axis designs?

In case of on-axis (coaxial) imaging applications, rotationally symmetric lenses are omnipresent as they greatly simplify the design and analysis of optical systems and the manufacturing process. The rotational symmetry of the optical system makes it the best solution for design problems where the object and image are rotationally symmetric with respect to the optical axis.

However, from a pure symmetry point of view, a rotationally symmetric system is clearly mismatching the rectangular dimensions of commonly used image sensors. Figure 2 (left) illustrates this ”field mismatch” for a rotationally symmetric optical design. By using free-form optics, the object points for which good image quality is targeted (designed field) could be reallocated to match the dimensions of the sensor; this is illustrated in Fig. 2 on the right.

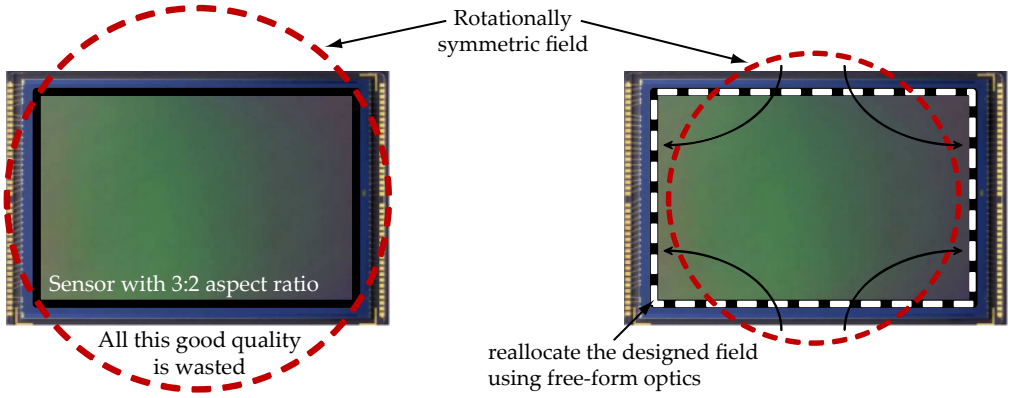

Fig. 2. (Left) The rotationally symmetric field for which the system is designed, is oversized for image sensors with rectangular aspect ratio. (Right) Any rotationally symmetric optical system for a rectangular field could be improved by making the surfaces free-form.

It becomes evident from Fig. 2 that any rotationally symmetric optical system could be improved by means of free-form optics - better matching the aspect ratio of a rectangular image sensor. In practice, a rotationally symmetric design approach is widely accepted sufficient for optical systems with rectangular image sensors characterized by moderate aspect ratios. However, with an increasing aspect ratio, the question if free-form optics might help to provide on-axis solutions with clearly enhanced performance becomes more and more interesting.

To evaluate the potential benefits of free-form optics in on-axis imaging applications with high aspect ratio, an optical design strategy is introduced in Sec. 2 that allows for a reliable evaluation and comparison of the imaging performance. In Sec. 3, the imaging performance for a field of view with high aspect ratio is compared for basic rotationally symmetric and free-form lenses. The performed analysis shows that the free-form lens provides superior imaging performance for applications with high aspect ratio, compared to conventional rotationally symmetric systems. Finally, in Sec. 4, conclusions are drawn and an outlook is given.

#200472 - $15.00 USD Received 31 Oct 2013; revised 26 Nov 2013; accepted 26 Nov 2013; published 9 Dec 2013

2. Optical design approach for imaging applications with high aspect ratio

Figure 3 (left) illustrates the strong "field mismatch" of a rotationally symmetric optical design for an image sensor with high aspect ratio. For such high aspect ratios, one possible design strategy is to start from a rotationally symmetric lens and reallocate the designed field using free-form optics. However, the achievable performance improvement through optimization depends on the chosen initial design and does not necessarily lead to satisfactory results. To reliably assess the potential benefits of free-form optics in such a case, the imaging performance for an object at infinity of two basic thick lenses (each consisting of two surfaces) are compared in this work. The rotationally symmetric reference design is shown in Fig. 3 in the middle, the free-form lens design is shown on the right. The surfaces of both lenses are calculated using an analytic optics design method that we have developed recently.

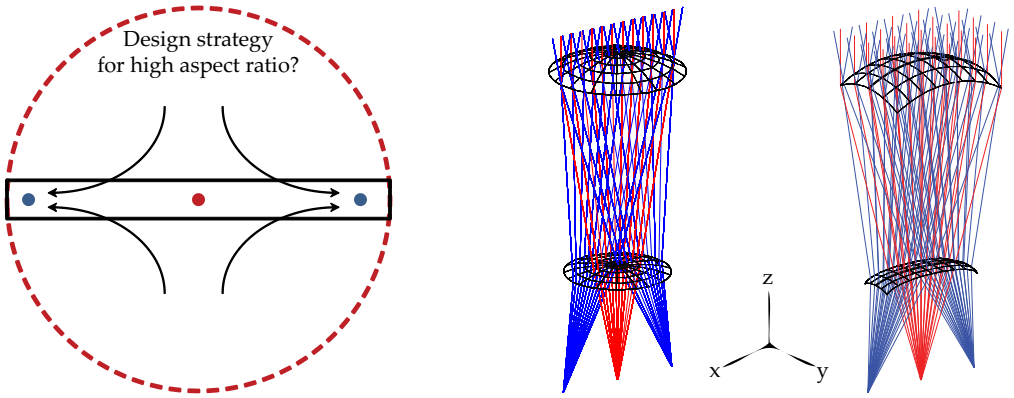

Fig. 3. (Left) A rotationally symmetric field is clearly mismatching a rectangular receiver with high aspect ratio. (Right) The free-form lens seems as a very promising solution to better suit the desired aspect ratio than a classic rotationally symmetric lens.

Similar to the SMS design method [12], the analytic design method only controls individual field points over the full field of view. For a more general formulation of the SMS2D design method for imaging systems, it was shown that the obtained image quality over the entire field of view is superior when compared with equivalent aplanatic designs [13]. Since then, the SMS2D design method has been used to design several imaging systems [14–16], underlining the potential of such a design approach.

The two-dimensional analytic design method allows to couple three ray-bundles using two free-form lens profiles - one ray-bundle more than with the SMS2D design method [17]. The rotationally symmetric lens is then obtained by rotating the lens profiles around the optical axis. Due to the rotational symmetry, the lens will perfectly image parallel rays with incident angle $0°$, but not the skew rays with incident angles $\pm\theta$.

The free-form lens (right figure) is calculated using the generalized 3D version of the analytic design method [18]. It perfectly images three (parallel) ray-bundles with incident angles $0°$ and $\pm\theta$ onto three image points. Its cross section in x-z-plane (the thicker lines in the right figure) is given by the two-dimensional design method as a partial solution to the full three-dimensional problem. Both lenses thus form an image of an object at infinity. The analytic free-form solution with its aberration free imaging for three specific image points (marked in Fig. 3 on the left) along a line will serve as a very good starting point for such a high aspect ratio free-form imaging system. Furthermore, the analytic design approach in two and three dimensions enables a direct and objective comparison of the imaging performance of the free-form lens with its equivalent rotationally symmetric counterpart.

#200472 - $15.00 USD Received 31 Oct 2013; revised 26 Nov 2013; accepted 26 Nov 2013; published 9 Dec 2013

2.1. *Implementation and spot diagram analysis*

To compare the imaging performance of both lenses, a common initial off-axis design angle and refractive index (θ, n_2) are selected as input parameters for the analytic optics design method for both lenses with values $(11°, 1.5)$. The imaging performance of both systems is evaluated using Synopsys' *Code V*. As *Code V* (Version 10.5) does not support the direct implementation of general Taylor polynomials centred at an arbitrary point $x_0 \neq 0$, the derived analytic solutions had to be remodelled. Therefore, the coefficients of the aspherical surfaces according to their definition in *Code V* are fitted to the calculated two-dimensional analytic lens profile solutions, using an approximation algorithm of least squares in MATLAB. The determined aspherical coefficients up to 18^{th} order can now be directly imported into *Code V* and used to define the circular rotationally symmetric lens. A 3D viewing of ray tracing for the circular rotationally symmetric lens is shown in Fig. 4 on the left.

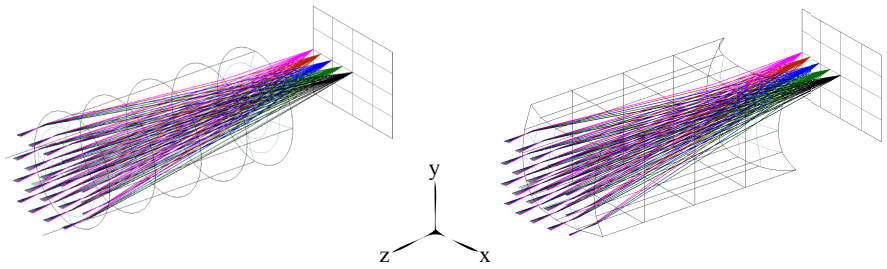

Fig. 4. 3D viewing of ray tracing for the circular rotationally symmetric lens on the left, and the rectangular free-form lens on the right, after conversion to *Code V* surfaces.

The three-dimensional free-form lens surfaces are fitted to XY Polynomial surfaces (SPS XYP) using a similar approximation method of least squares in MATLAB. The SPS XYP surface is defined by a series of polynomials (up to the 10^{th} order) added to a base conic and the polynomial is expanded into monomials of $x^n y^m$, with $(m+n) \leq 10$. This order is lower than the order provided 15^{th} by the analytic solution. However, it is still sufficiently high, which can be seen from the spot diagram in Fig. 6 on the right. Due to the quadrant symmetry of the free-form lens, "only" 20 coefficients for each lens surface do not equal zero. A 3D viewing of ray tracing for the free-form lens is shown in Fig. 4 on the right. To better illustrate the actual lens' shapes, Fig. 5 shows the *x*-*z*- and *y*-*z*-plane cross-section profiles of the two lenses for the first (left) and second (right) surfaces.

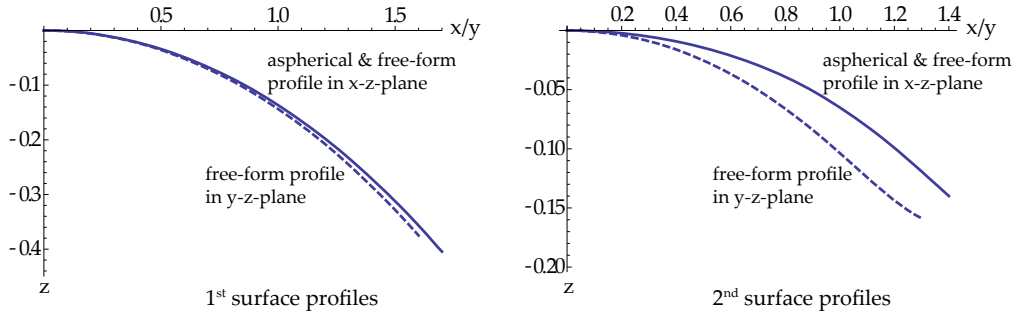

Fig. 5. Comparison of the in-plane cross-section profiles of the two lenses: the profiles of the aspherical lens and the free-form lens in *x*-*z*-plane coincide, whereas the (dashed) profiles of the free-form lens in *y*-*z*-plane clearly deviate from the aspherical profiles.

#200472 - $15.00 USD Received 31 Oct 2013; revised 26 Nov 2013; accepted 26 Nov 2013; published 9 Dec 2013

As the analytic two-dimensional design provides a partial solution to the full three-dimensional design problem, the profiles of the aspherical lens and the free-form lens in x-z-plane coincide. The profiles of the free-form lens in y-z-plane clearly deviate from the aspherical profiles.

The circular entry aperture diameter of the rotationally symmetric lens measures 3.4 mm. The imaging performance of the rotationally symmetric system does not seem to benefit from an elliptical pupil as long as the surface area of the entry aperture is kept constant. This has been tested for different elliptical pupils with five eccentricity values between 0.4 and 0.8. The free-form lens has a rectangular entry aperture of 2.84 mm$\times$3.2 mm to result in identical entrance aperture sizes lenses for a fair comparison. The f-number of the rotationally symmetric lens is $f/2.7$. In general, a free-form lens cannot be described by a single f-number. Here, the f-number is $f/2.8$ in x-direction, and $f/3.0$ in y-direction.

To verify the line imaging performance of both lenses, the spot diagrams for different field positions along the x-axis (see Fig. 4) are shown in Fig. 6 for the rotationally symmetric lens (left) and the free-form lens (right). The added black circles to the spot diagrams correspond

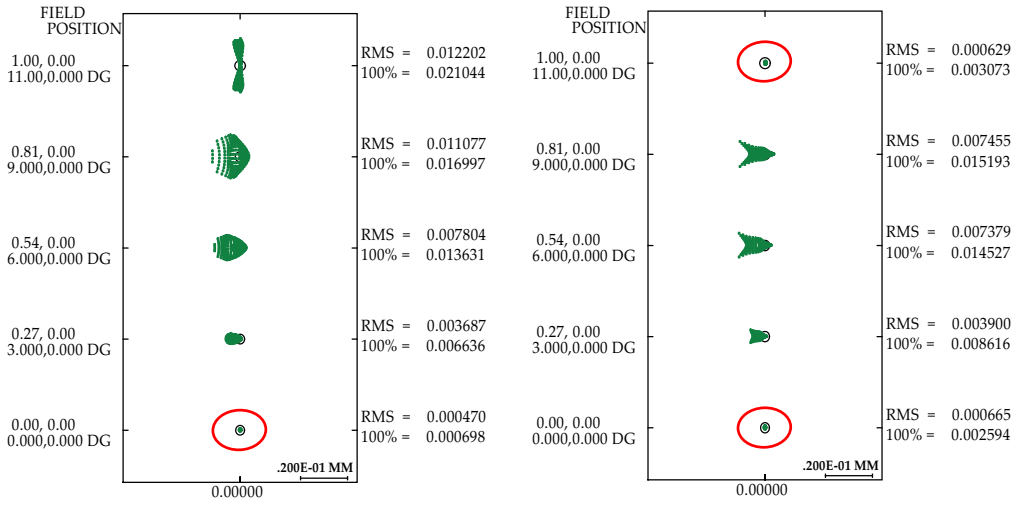

Fig. 6. Spot diagrams for the circular rotationally symmetric lens (left), and for the rectangular free-form lens (right). As expected from the design characteristics, the RMS spot diameters are minimal at the design angles $\pm 11^\circ$ and 0° for the 3D free-form design, and at 0° for the rotationally symmetric lens, highlighted in red.

to the Airy disk diameters (determined from real ray tracing) at the reference wavelength for refractive index $n_2 = 1.5$. In both cases, the dimensions of the lower lens surface are chosen to match the dimensions of the entrance aperture to ensure that all rays entering the lens also reach the image plane. As expected from the design characteristics, the RMS spot diameters at the design angle 0° in case of the rotationally symmetric lens and at the design angles 0° and 11° in case of the free-form lens are very close to zero (of the order of 0.5 micrometers), free from aberrations (like e.g., coma) and lie within the Airy disk diameters.

In direct comparison, the analysis for intermediate incident directions demonstrate a considerably better overall line imaging performance for the free-form lens when compared with its rotationally symmetric counterpart both for the RMS values, as well as for the 100% spot diameters.

#200472 - $15.00 USD Received 31 Oct 2013; revised 26 Nov 2013; accepted 26 Nov 2013; published 9 Dec 2013

3. Free-form optics for a field of view with high aspect ratio

To start with, the imaging performance is evaluated for the same systems as in the previous section. The RMS spot diameter field maps are calculated with *Code V* for a $26^\circ \times 5^\circ$ field of view. These values might appear arbitrary, but they ensure that for both the analytic rotationally symmetric and the free-form lens design, all rays passing through the first lens surface still reach the image plane. Due to the systems' symmetries, it is sufficient to analyse only a quadrant of the full field of view. Figure 7 shows the calculated contour plots of the RMS spot diameter distributions for the analytic rotationally symmetric lens (top), and for the free-form lens design (bottom). These plots provide a very good first insight into how differently the contour lines are distributed.

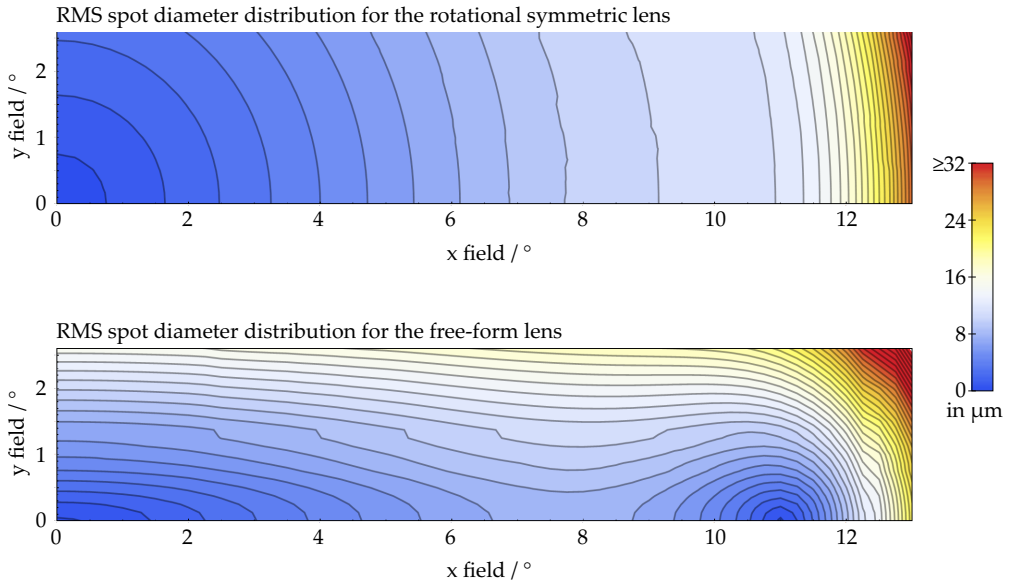

Fig. 7. The comparison of the RMS spot diameter contour plots for the circular rotationally symmetric lens (top) and for the rectangular free-form lens (bottom) illustrate the very different allocation of the designed fields.

In case of the rotationally symmetric lens, the RMS spot diameter distribution is also rotationally symmetric. This means that for a field of view with very high aspect ratio, the imaging performance deviates only slightly from a line imaging system: it is mainly dominated by the x-field dependency of the RMS spot diameter distribution. The situation is very different for the case of the free-form lens. The contour lines of the RMS spot diameter distribution can essentially be divided into two main regions. Almost horizontal contour lines for larger y field angles, and (curved) vertical contour lines beyond the off-axis design angle of 11°, forming approximately rectangular contour lines for this RMS spot diameter distribution.

3.1. Optimization strategy and results for a 10:1 field of view

The analytic lens designs can be optimized to find better solutions with lower and more balanced RMS spot diameter distributions over a given field of view. The monochromatic optimization is carried out using the "Automatic Design" option in *Code V*. This optimization option varies all permitted variables in a lens design simultaneously, so that the lens is improved in terms of the defined performance merit function. *Code V* uses a damped least squares

#200472 - $15.00 USD Received 31 Oct 2013; revised 26 Nov 2013; accepted 26 Nov 2013; published 9 Dec 2013

(DLS) algorithm for optimization, which is very effective at finding a local minimum. The image defects are described by transverse ray aberrations, the default error function of *Code V*. This function measures the transverse displacements Δx and Δy of all traced skew rays from the ideal image point, which is calculated by the intersection of the chief ray with the image plane [19]. The Automatic Design option is used with the default Transverse Ray Aberration merit function to find better solutions for both lens systems for a $24° \times 2.4°$ (10:1 aspect ratio) FOV. In both cases, the field is divided into a grid of six equidistant angles in *x*-, and three equidistant angles in *y*-direction. Only the aspherical and polynomial coefficients describing the lens surfaces are permitted as variables to optimize the RMS spot diameters across the field of view, while the surface vertices are kept constant. If this is not the case, the optimization process seems to fail and it results in much worse imaging performance than the initial analytic solutions provided. The impact of varying the weighting factors for each field point of the merit function has been thoroughly tested for both optimizations. The best results have been achieved with a merit function for which the weighting factors of the sampled field points increased with the field angle. For these specific settings, the optimization of both lenses converges very well within a few cycles and the image quality for both designs is considerably improved.

Figure 8 shows the contour plots of the RMS spot diameter distributions for the optimized rotationally symmetric lens (top) and the optimized free-form lens (bottom). The targeted field of view is marked by an additional rectangle in both plots. For the 10 : 1 FOV, the RMS spot diameter values of the optimized rotationally symmetric lens range from 3 to 11 micrometers.

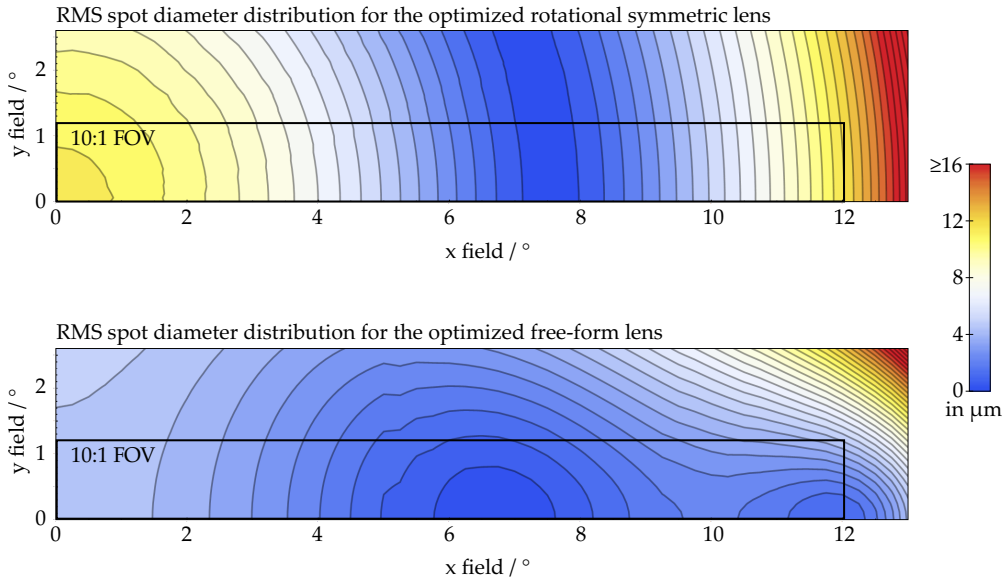

Fig. 8. RMS spot diameter contour plots for the circular rotationally symmetric lens (top) and the rectangular free-form lens (bottom) after optimization for the indicated 10:1 FOV. The figures clearly show the superior imaging performance of the free-form lens in terms of RMS spot diameter, compared with the rotationally symmetric lens.

A clear improvement in comparison to 0.4 to 17 micrometers in case of the unoptimized analytic rotationally symmetric lens design. The RMS spot diameter distribution of the optimized free-form lens sees a shift and attenuation of the former sharp foci. The RMS spot diameter values range from 2 to 6 micrometers, compared with 0.5 to 14 micrometers in case of the unoptimized analytic free-form lens design and for the identical 10 : 1 field of view.

#200472 - $15.00 USD Received 31 Oct 2013; revised 26 Nov 2013; accepted 26 Nov 2013; published 9 Dec 2013

To illustrate the deviation of the free-form lens from its rotationally symmetric counterpart, Fig. 9 shows the surface contour plots of the first (left) and second (right) lens surface where the optimized rotationally symmetric surfaces are subtracted from the optimized free-form lens surfaces.

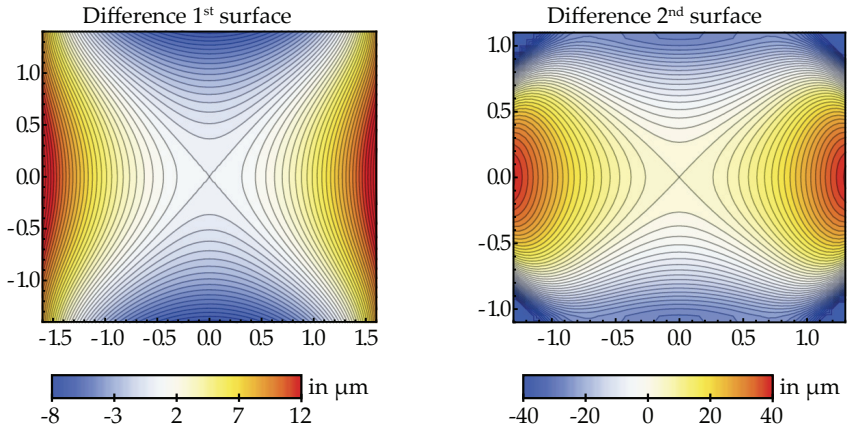

Fig. 9. Surface contour plots of the first (left) and second (right) lens surface where the optimized rotationally symmetric surfaces are subtracted from the free-form lens surfaces.

In direct comparison, the overall imaging performance in terms of RMS spot diameters of the optimized free-form lens clearly exceeds the performance of the optimized rotationally symmetric lens; almost by a factor of two for the specified field of view with a 10:1 aspect ratio. This result, however, is less about the absolute values itself. In fact, it clearly highlights the potential use of free-form optics for on-axis imaging applications, where the specified field of view is far from being circular symmetric. As a rule of thumb, the image quality improves linearly with the number of lenses and a rotationally symmetric asphere allows the removal of one lens [20]. Interestingly, this implies for the system of interest that two free-form lens surfaces would perform as well as three rotationally symmetric aspheres, or six spherical lens surfaces.

4. Conclusion

Compact off-axis imaging designs have already demonstrated the added value of free-form surfaces for imaging applications. Maybe less obvious but not less important is the potential of free-form solutions for on-axis imaging or related applications.

The evaluated imaging performance for a field of view with 10:1 aspect ratio demonstrates the superiority of the free-form lens solution when compared with its rotationally symmetric counterpart. For an extended field of view with 10:1 aspect ratio, the overall imaging performance of the optimized free-form lens exceeds the performance of the optimized rotationally symmetric lens almost by a factor of two. Particularly noteworthy is the low variation of the RMS spot diameters of the optimized free-form lens over the entire field of view.

Such high aspect ratios can be interesting for special applications like fluorescence imaging, machine vision (inspection and safety) or laser materials processing. In contrast to often used combinations of rotationally symmetric plus anamorphic elements like cylindrical lenses, free-form optics offer the possibility of symmetry matching solutions with the potential to reduce the number of needed lenses. Even for the very common and moderate 16:9 aspect ratio HD standard in imaging systems, it seems reasonable to assume that the optical system design will also benefit from tailor-made free-form optics.

#200472 - $15.00 USD Received 31 Oct 2013; revised 26 Nov 2013; accepted 26 Nov 2013; published 9 Dec 2013

This sensor type becomes increasingly popular in point-and-shoot cameras and also in cell phone cameras with very few optical elements and little space. However, for such moderate aspect ratios, the question remains if the potential increase in the image performance justifies the higher manufacturing complexity and costs of free-form optics.

To investigate such systems, it would be very important to increase the number of optical surfaces that can be calculated with direct free-form design methods and to add an aperture stop; which has been recently shown for a single optical surface imaging design with object to image mapping [21]. These are possible optical design questions to be addressed in future work.

Acknowledgments

The work reported in this paper is supported in part by the Research Foundation - Flanders (FWO-Vlaanderen) that provides a post-doctoral grant to Fabian Duerr, and in part by the IAP-BELSPO grant IAP P7-35 photonics@be, the Industrial Research Funding (IOF), Methusalem, and the OZR of the Vrije Universiteit Brussel.

#200472 - $15.00 USD Received 31 Oct 2013; revised 26 Nov 2013; accepted 26 Nov 2013; published 9 Dec 2013